

Sea Breeze, Coastal Upwelling Modeling to Support Offshore Wind Energy Planning and Operations

Greg Seroka, Travis Miles, Rich Dunk, Josh Kohut, Scott Glenn
Center for Ocean Observing Leadership
Rutgers University
New Brunswick, NJ USA
seroka@marine.rutgers.edu

Erick Fredj
The Jerusalem College of Technology
21 Havaad Haleumi St., P.O. Box 16031
Jerusalem 91160, Israel

Abstract— In July 2014, BOEM issued the NJ Proposed Sale Notice of nearly 344,000 acres designated for offshore wind (OSW) energy development. The BOEM lease auction is expected to take place during the current year. The OSW developer(s) who win the lease(s) will submit their development application to the NJ Board of Public Utilities (NJ BPU). These applications must include a wind resource assessment and economic analysis.

One major focus in the NJ BPU OSW rules is that applications “shall account for the coincidence between time of generation for the project and peak electricity demand.” Preliminary data analysis shows two mesoscale processes—coastal upwelling and sea breeze—may have a significant impact on wind generation during peak electricity demand. Tasked by NJ BPU, the Rutgers University Center for Ocean Observing Leadership (RUCOOL) is using the Weather Research and Forecasting (WRF) model to resolve these processes and quantify their impact on the wind resource.

The WRF model set-up used is designed specifically for coastal/offshore regions, with three pertinent features for these regions. First, innovative satellite sea surface temperature (SST) composites at 2km resolution are used to resolve coastal upwelling. These composites integrate a) our own declouding algorithm set for the Mid Atlantic Bight to remove cloudy pixels from Advanced Very High Resolution Radiometer (AVHRR) SST scans, and b) coldest pixel composites of the resulting declouded AVHRR SST scans, rather than warmest pixel composites that would effectively remove coastal upwelling. Second, microscale grid spacing (<1km) is used in WRF to resolve the sea breeze circulation, which can vary at meso- to microscales. Finally, validation of the WRF simulations is performed against coastal/offshore wind monitoring sites with atmospheric heights up to 200m, in order to ensure adequate model performance in coastal/offshore conditions.

Three main results will be presented in this paper:

- (i) Coastal upwelling can produce high wind shear ($\sim 8 \text{ ms}^{-1}$ across rotor blade dimensions). These significant shear values could potentially pose engineering challenges and should be considered in wind resource assessments.

- (ii) Lagrangian Coherent Structure (LCS) methodology can be used to identify key boundaries and fronts within the sea breeze circulation. While the onshore component of the sea breeze is well observed, very little is known about its unobserved offshore component, where OSW turbines will be installed.

- (iii) Power generation from a hypothetical 3000 MW OSW scenario off NJ was analyzed during three different sea breeze cases (one with strong upwelling, one with weak upwelling, and one without upwelling). Significant variability in power production occurred within each case and across the three sea breeze cases (net capacity factor ranged from 1 to 95%).

WRF OSW potential power production data are being ingested by an electricity grid model to evaluate the impact of OSW energy penetration into the electrical power grid along with evaluating the economic portion of the applications. NJ is leading development of such an advanced joint atmospheric-economic modeling capability for determining the viability of OSW projects.

Ongoing work includes development of a coupled atmosphere-ocean model (WRF-ROMS, Regional Ocean Modeling System), which will provide improved capabilities to diagnose coastal air-sea processes (sea breeze and coastal upwelling) for OSW resource assessment (i.e. lowering uncertainty by including relevant mesoscale processes in simulations), and to more accurately predict these processes for operational forecasting during OSW construction and O&M phases.

Index Terms—Offshore wind energy, sea breeze, coastal upwelling, numerical modeling, atmospheric modeling, WRF, coastal processes, wind resource assessment, Lagrangian Coherent Structures, LCS, net capacity factor, power production

I. INTRODUCTION

The BOEM lease auction for offshore wind (OSW) in New Jersey (NJ) is expected to take place during the current year (2015). The OSW developer(s) who win the lease(s) will submit their development application to the NJ Board of Public

Utilities (NJ BPU). These applications must include a wind resource assessment and economic analysis of proposed project(s).

The NJ BPU OSW rules requires OSW developers to “account for the coincidence between time of generation for the project and peak electricity demand”, in their applications to develop OSW off NJ. Two different coastal mesoscale processes—coastal upwelling and sea breeze—may have a significant impact on wind generation during peak electricity demand periods. Tasked by NJ BPU, the Rutgers University Center for Ocean Observing Leadership (RUCOOL) is using the Weather Research and Forecasting (WRF) model to resolve these processes and quantify their impact on the wind resource.

The WRF model set-up used is designed specifically for coastal/offshore regions, with three pertinent features for these regions. First, innovative satellite sea surface temperature (SST) composites at 2km resolution are used to resolve coastal upwelling. These composites integrate a) our own declouding algorithm set for the Mid Atlantic Bight to remove cloudy pixels from Advanced Very High Resolution Radiometer (AVHRR) SST scans, and b) coldest pixel composites of the resulting declouded AVHRR SST scans, rather than warmest pixel composites that would effectively remove coastal upwelling. Second, microscale grid spacing (<1km) is used in WRF to resolve the sea breeze circulation, which can vary at meso- to microscales. Finally, validation of the WRF simulations is performed against coastal/offshore wind monitoring sites with atmospheric heights up to 200m, in order to ensure adequate model performance in coastal/offshore conditions.

We aim to answer three questions in this paper:

- (i) What effect does cold coastally-upwelled water (e.g. Fig. 1) have on the coastal/offshore wind resource?

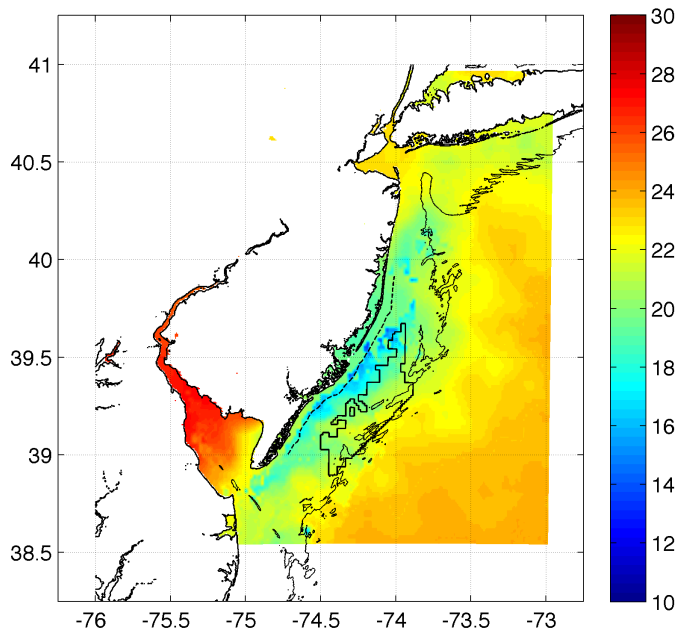


Fig. 1: Coastal upwelling example on July 7, 2013. Sea surface temperature (SST) is plotted in color. The NJ Wind Energy Area (WEA) grid is plotted in

black, and the 30m isobaths is also plotted in black. State-federal water boundary at 3 nmi offshore is plotted in dashed black.

- (ii) What does the offshore component of the sea breeze look like? Is there a secondary circulation offshore and an area of divergent light wind in the coastal zone (Fig. 2)?

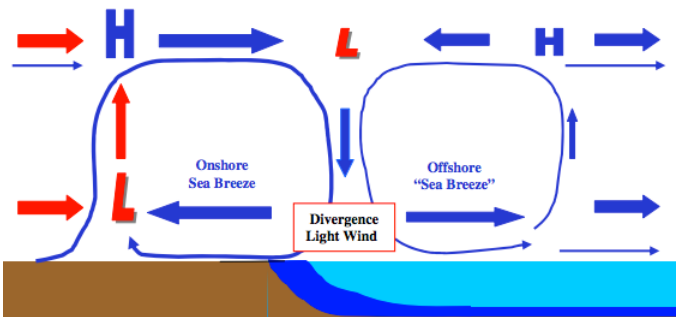


Fig. 2: Hypothesis of the onshore and offshore sea breeze. The onshore sea breeze is well observed but the offshore component is not, and thus more unknown.

- (iii) How does OSW power generation vary within a sea breeze and between one sea breeze and another?

II. METHODS

A. Coastal upwelling sensitivity

To answer the first question listed in the introduction, we conducted two nested WRF v 3.6.1 simulations, with an outer nest at 3km resolution and inner nest at 600m resolution. We focus on a sea breeze case that occurred on July 31, 2014, with very weak coastal upwelling (Fig. 3). The first simulation was using the SST conditions that naturally occurred for this case (Fig. 3), and the second simulation was using the intense coastal upwelling that occurred on July 7, 2013 (Fig. 1).

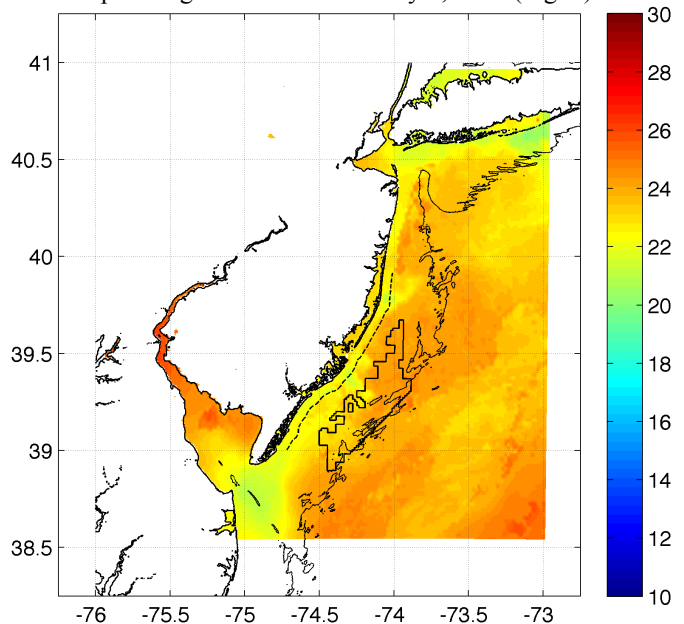


Fig. 3: Very weak coastal upwelling on July 31, 2014.

Traditional SST composites remove coastal upwelling because the declouding algorithms (often a warmest pixel composite) think the cold upwelled water is cloud. We use our own innovative satellite SST composite which resolves coastal upwelling using a coldest dark pixel compositing technique [1].

B. Lagrangian Coherent Structures and offshore sea breeze

Unsteady flow fields, as we find in the coastal and open ocean and atmosphere, typically have a mixture of Coherent Structures (CSs), jets, and mixing layers that move in an unsteady fashion, and typically exist only for some finite time. Roughly, by coherent structure, we mean a body of fluid that moves together for a certain period of time in any reference frame one chooses; namely, we take the Lagrangian point of view which is frame independent. Passive particles (such as atmospheric dust) placed inside such a coherent structure remain in it as long as it lives, often moving roughly quasi-periodically around the coherent structure center.

Broadly, Lagrangian Coherent Structures (LCSs) are boundaries in a fluid that distinguish regions of differing dynamics [2]. LCSs are often associated with filaments and mesoscale features, such as eddies, jets and fronts. These boundaries limit material transfer between air parcels and act as mixing boundaries. Particles aggregate and move along attracting LCSs (aLCSs) and move away from and along a repelling LCS (rLCS) (Fig. 4). Thus, aLCSs map lines where atmospheric particles can be both aggregated and transported.

Computation of LCS therefore can identify regions of convergence and divergence within a fluid flow—in our case, the sea breeze. Numerous ways to identify LCSs have been proposed in recent years, including finite time Lyapunov exponent (FTLE), finite size Lyapunov exponent (FSLE), or relative dispersion (RD).

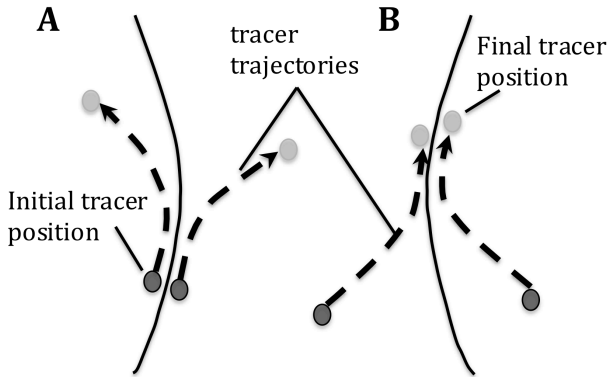


Fig. 4: Behavior of tracers near attractive Lagrangian coherent structure (aLCS) curves (solid lines). As time progresses forward, the position of 2 initially adjacent tracers on either side of a repelling LCS diverge (Panel A). For 2 tracers initially on either side of an attracting LCS (Panel B), as time progresses forward their positions converge on the attracting LCS curve. Dashed gray curves: tracer trajectories with arrows indicating direction; dark and light gray circles: initial and final tracer positions, respectively.

Let us define $R(t) = \|r^{(1)} - r^{(2)}\|$ as the distance between two trajectories at time t . RD is defined as the second order moment of $R(t)$

$$\langle R^2(t) \rangle = \langle \|r^{(1)} - r^{(2)}\|^2 \rangle$$

where the average is over all the available trajectory pairs $(r^{(1)}, r^{(2)})$.

In the small-scale range, the velocity field between two sufficiently close trajectories is reasonably assumed to vary smoothly. This means that, in nonlinear flows, the particle pair separation typically evolves following an exponential law:

$$\langle R^2(t) \rangle \sim e^{L(2)t}$$

where $L(2)$ is the Generalized Lyapunov Exponent of order 2. When fluctuations of the finite time exponential growth rate around its mean value are weak, one has $L(2) \approx 2\lambda_L$, where λ_L is the Lagrangian Maximum Lyapunov exponent (MLE). Notice that for ergodic trajectory evolutions the Lyapunov exponents do not depend on the initial condition. If $\lambda_L > 0$ (expect for a set of zero probability measure) we speak of Lagrangian chaos. The chaotic regime holds as long as the trajectory separation remains sufficiently smaller than the characteristic scale's motions.

In the opposite limit of large particle separations, when two trajectories are sufficiently distant from each other to be considered uncorrelated, the mean square relative displacement behaves as:

$$\langle R^2(t) \rangle \sim 4K_E t, \text{ for } t \rightarrow \infty$$

where K_E denotes the asymptotic eddy-diffusion coefficient. At any time t , the diffusivity $K(t)$ can be defined as:

$$K(t) = \left\langle \frac{1}{4} \frac{dR^2}{dt} \right\rangle = \frac{1}{2} \langle R(t) \frac{dR}{dt} \rangle \text{ with } K(t) \rightarrow K_E \text{ for } t \rightarrow \infty$$

If several scales of motion characterize the velocity field, RD in the intermediate range (between the smallest and the largest characteristic length) depends on the properties of local velocity differences.

We use RD to characterize the persistent areas of offshore divergence and convergence in a WRF model simulation (3km) of a sea breeze that occurred on April 27, 2013.

C. Sea breeze and OSW power generation

To determine OSW power generation over the NJ WEA during sea breeze occurrences, we run the same WRF configuration (3km, 600m) for three sea breeze events: April 27, 2013 (no upwelling), July 7, 2013 (strong upwelling), and July 31, 2014 (weak upwelling). We construct a hypothetical 3000 MW wind farm in the NJ WEA using a generic 6 MW wind turbine power curve, which is a combination of several newer 6 MW wind turbine models available today, as well as two different array spacings: 10X12 (Fig. 5 as an example) and 10X15 rotor diameter spacing.

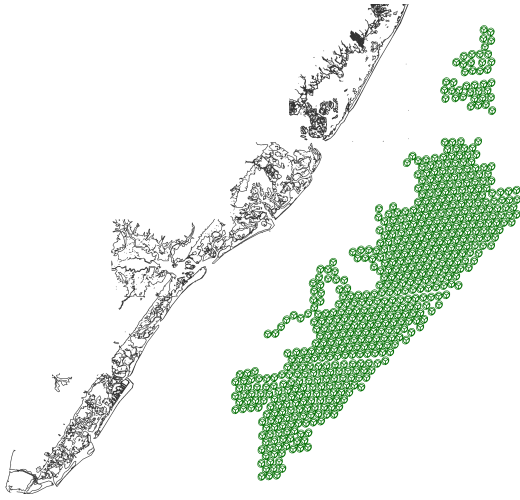


Fig. 5: Hypothetical 3000MW wind turbine array using 10X12 spacing. Each green oval represents a 6 MW OSW turbine within NJ WEA.

For each of the sea breeze cases, we determine hourly wind speed averaged across the wind farm, hourly potential power production (MWh), and hourly net capacity factor (NCF) using the hypothetical turbine arrays and output from the WRF simulations.

III. RESULTS

A. Coastal upwelling increases 100m hub height winds, but also increases wind shear

SST difference between the two 600m simulations of the July 31, 2014 sea breeze case is shown below in Fig. 6A (the same as the difference between Fig. 1 and 2). Differences are widely -4 to -5°C offshore NJ due to the presence of intense coastal upwelling from July 7, 2013 (Fig. 1) and only weak upwelling on July 31, 2014 (Fig. 3).

Fig. 6B shows the average hourly (across 30 hours of simulation) difference in 10m wind speeds between the two runs. Coincident over the negative difference in SST (over the coastal upwelling) are negative differences in 10m wind speeds offshore, up to -1 m/s. The same is shown in Fig. 6C but for 100m hub height wind speeds, where large positive differences are coincident over the upwelling core offshore NJ, again with values up to ~ 1 m/s. The r^2 value between the SST difference (Fig. 6A) and 10m wind speed difference (Fig. 6B) is 0.61, and the r^2 value between the SST difference (Fig. 6A) and 100m wind speed difference (Fig. 6C) is 0.58.

A vertical cross section through the northern half of the NJ WEA and through the core of the coastal upwelling shows the vertical extent of the negative and positive differences (Fig. 6D). From the surface up to about 60m in the atmosphere, wind speed differences are negative over the upwelled waters. From about 60m to 200m+, wind speed differences are positive. If a hub height of 100m is assumed for OSW turbines, then the blade swept rotor diameter would stretch from about 40m to 140m above sea level. Therefore, although 100m hub height wind speeds actually increased due to the insertion of coastal upwelling in the WRF simulation, wind shear across the wind turbine blade increased as well. Hourly wind shear values

increased up to ~ 8 m/s across the wind rotor blade dimensions (not shown). These significant shear values could potentially pose engineering challenges and should be considered in wind resource assessments.

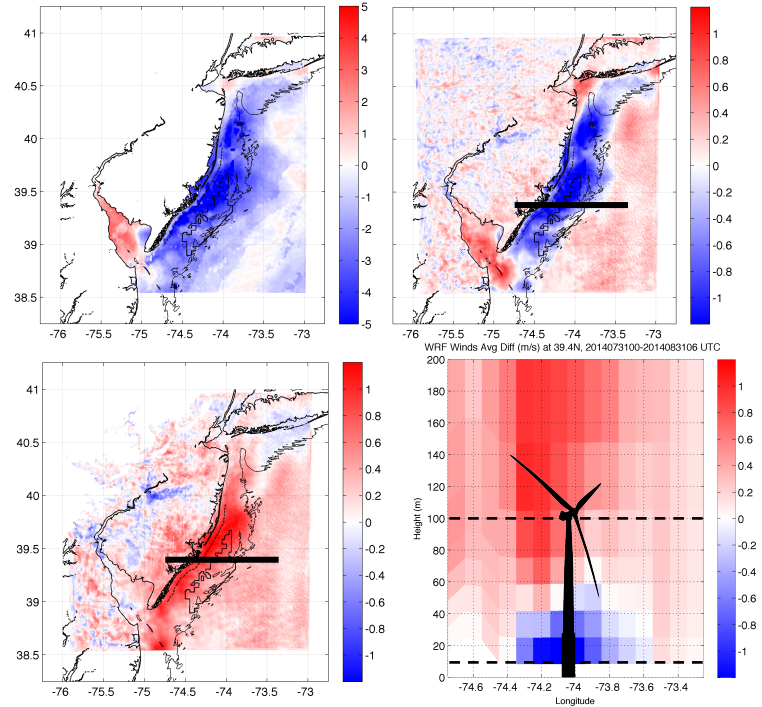


Fig. 6: A (top left): SST difference ($^{\circ}\text{C}$) between July 7, 2013 intense coastal upwelling and July 31, 2014 weak upwelling. B (top right): Average hourly 10m wind speed difference between model simulations with SSTs differenced in A. C (bottom left): Same as B but for 100m wind speeds. D (bottom right): Cross section through black line indicated in B and C, with typical wind turbine dimensions plotted and dashed lines indicating heights of winds plotted in B and C.

B. Using LCS to quantify size of offshore and onshore sea breeze cells

For the April 27, 2013 sea breeze case, we took the WRF 3km resolution simulated winds from 1800 to 2300 UTC. Trajectories of parcels, and then LCSs of those trajectories were computed at 10, 50, 100, 150, 500, 1000, 1500, 2000, and 2500m above ground level (AGL). As stated above, one way to identify and quantify LCSs is by using relative dispersion (RD). If a region in the field has high RD, then it means that region is characterized by divergent flow. If a region has low RD, then the region has convergent flow, relatively speaking.

Fig. 7 shows RD computed at 500m AGL. The NJ WEA—the area of interest—is depicted in the black box southeast of the NJ coast. High values of RD—and thus divergence at this level—are present in the Delaware Bay, and the regions just offshore of NJ, including over the NJ WEA. Low values of RD—and thus convergent flow—are present over inland areas of NJ. Although 500m was chosen for this paper, all levels below 500m depict the same general spatial pattern of RD.

Fig. 8 shows RD computed at 1000m AGL. Almost the complete opposite pattern of RD occurs at this level. High RD values are shown for onshore regions of NJ, whereas relatively

lower values of RD are present offshore of NJ, over the NJ WEA.

These results confirm what was hypothesized in Fig. 2 above—at the surface, divergent wind over offshore winds near the coast, and at some level higher up in the atmosphere, convergent winds above the surface divergent winds. Further, the vertical scale of the onshore and offshore sea breeze cells can also now be quantified. The abrupt switch in RD between 500m and 1000m AGL shows that both the onshore and offshore sea breeze cells extend from the surface up to about 500-1000m AGL. Further analysis is needed to pinpoint this exact vertical level, as well as to determine the horizontal extent of the offshore sea breeze cell.

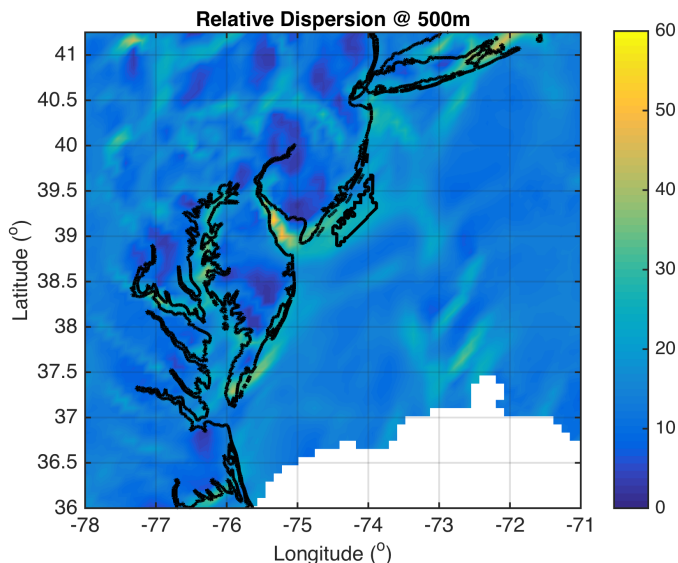


Fig. 7: Relative dispersion (RD) at 500m above ground level (AGL) calculated from the LCS of the WRF 3km simulated winds for the April 27, 2013 sea breeze, from 1800 to 2300 UTC.

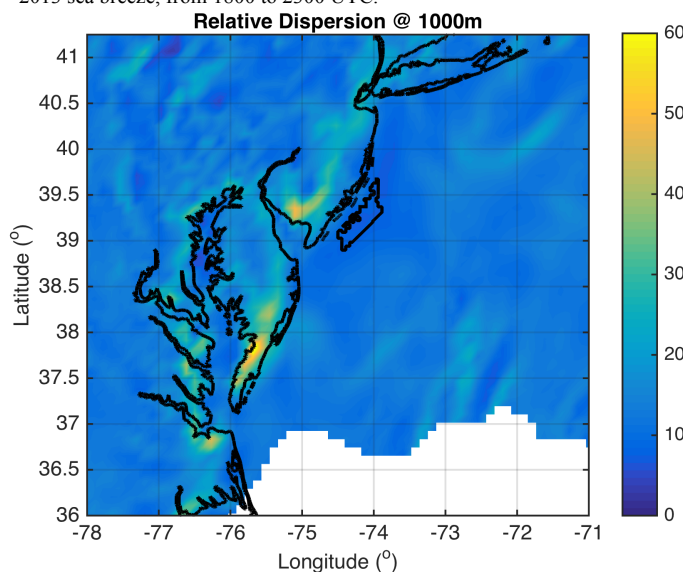


Fig. 8: Same as Fig. 7, but at 1000m AGL.

C. Net capacity factor can vary significantly within a sea breeze, and between one sea breeze case and another

Table 1 below shows hourly data from the July 7, 2013 sea breeze case (strong upwelling) using WRF 3km output from the hypothetical 3000MW offshore wind farm, using the 10X12 turbine spacing scenario. Significant hourly variability in net capacity factor (NCF) is present, with values ranging from 33% to 95%. From 12 to 13 EST, NCF sharply increased from 38% to 73%.

Date	EST	Avg WS	MWh	NCF
7/6/13	20	10.29	1860	62%
7/6/13	21	11.36	2343	78%
7/6/13	22	11.80	2482	83%
7/6/13	23	13.76	2773	92%
7/7/13	0	12.90	2728	91%
7/7/13	1	11.62	2416	81%
7/7/13	2	11.10	2297	77%
7/7/13	3	10.51	1950	65%
7/7/13	4	10.23	1848	62%
7/7/13	5	9.55	1544	51%
7/7/13	6	9.89	1670	56%
7/7/13	7	10.70	2051	68%
7/7/13	8	11.61	2431	81%
7/7/13	9	9.88	1625	54%
7/7/13	10	8.75	1181	39%
7/7/13	11	8.23	981	33%
7/7/13	12	8.58	1076	36%
7/7/13	13	8.69	1141	38%
7/7/13	14	10.93	2186	73%
7/7/13	15	12.51	2648	88%
7/7/13	16	13.33	2799	93%
7/7/13	17	14.69	2844	95%
7/7/13	18	15.44	2844	95%
7/7/13	19	15.83	2844	95%
7/7/13	20	15.51	2844	95%
7/7/13	21	14.42	2844	95%

Table 1: An example data table for the July 7, 2013 sea breeze case (using WRF 3km model data and 10X12 turbine spacing), showing hourly average wind speed calculated across the hypothetical 3000MW wind farm, MWh power production, and net capacity factor (NCF).

Finally, we took the average net capacity across all hours of simulation of each sea breeze case, for both the 3km and 0.6km resolution WRF runs and for the 10X15 and 10X12 turbine spacing scenarios. The spatial resolution of WRF did not significantly change NCF, likely because both resolutions of WRF effectively resolved, or captured, the sea breeze circulation. (Although higher spatial resolution for one case—the April 27, 2013 sea breeze—did significantly lower average NCF from about 16% down to about 12%). Further, the

turbine spacing also did not significantly affect the average NCF, because most of the time the winds were blowing in the “10” direction (from the SE or from the NW), rather than blowing in the “12” or “15” direction (from the SE or NE).

The most interesting result is that average NCF for each sea breeze case can vary from about 12% up to about 75%, depending on the synoptic wind conditions. A sea breeze circulation can form in very strong synoptic flow, which would lead to very high overall NCF, as in the July 7, 2013 case (with strong upwelling). On the other hand, a sea breeze can also form in very light synoptic flow conditions, as in the April 27, 2013 case without any upwelling. This would lead to lower average NCF.

Average Net Capacity Factors		
10x15	WRF resolution	Average NCF
20140731	3km	16.12%
20140731	0.6km	15.83%
20130707	3km	70.81%
20130707	0.6km	74.11%
20130427	3km	16.56%
20130427	0.6km	11.98%
10x12	WRF resolution	Average NCF
20140731	3km	16.33%
20140731	0.6km	16.06%
20130707	3km	72.12%
20130707	0.6km	75.48%
20130427	3km	16.37%
20130427	0.6km	11.83%

Table 2: Average Net Capacity Factor across each sea breeze case for both the 3km and 0.6 km resolution WRF runs, and for the 10X15 and 10X12 turbine spacing scenarios.

IV. CONCLUSIONS

Three distinct conclusions can be made from this study:

- (i) Coastal upwelling increases winds at 60m to at least 200m, decreases 10-60m winds, and increases wind shear across OSW turbine rotor blade dimensions (~40-160m). Hourly wind shear values across these OSW turbine rotor blade dimensions approach 8 ms^{-1} . These significant shear values could potentially pose engineering challenges and should be considered in wind resource assessments.

- (ii) Lagrangian Coherent Structures (LCSs) are used to confirm locations of surface divergence (offshore) and convergence (onshore) during a sea breeze circulation. Results also indicate that offshore surface divergence switches to convergence somewhere between 500 and 1000m above ground level (AGL), thus implying that the vertical extent of the offshore sea breeze cell is about that size.
- (iii) Power generation from a hypothetical 3000 MW OSW farm off NJ during three sea breeze cases (one with strong upwelling, one with weak upwelling, and one with no upwelling) was analyzed. Hourly power production within a sea breeze case can vary from 1 to 95%. Average net capacity factor (NCF) from one sea breeze case to another can vary from 12 to 75%, which is the result of the synoptic wind conditions in which the sea breeze circulation sets up. Turbine spacing did not significantly affect power generation during these sea breeze events, because prevalent wind directions were along the “10” rotor diameter spacing axis, rather than the “12” or “15” axis. WRF model resolution is hypothesized to have a more significant impact on power generation when comparing a resolution that does not capture the sea breeze circulation (perhaps >10km), with a resolution that does capture the sea breeze circulation (i.e. both 3km and 0.6km in this study).

ACKNOWLEDGMENTS

This work was funded by a grant from the New Jersey Board of Public Utilities: “Atmospheric/Oceanic Analyses and Predictions to Support the Wind Energy Development Application Process Defined in NJBPU’s Offshore Wind (OSW) Renewable Energy Rules (N.J.A.C. 14:8-6) and the Offshore Wind Energy Development Criteria Presented in the NJ Energy Master Plan: Phases I-III”.

REFERENCES

- [1] Seroka, G, R. Dunk, S. Glenn, L. Bowers, J. Kerfoot, M. Crowley, H. Roarty, L. Palamara (2012), Rutgers university coastal ocean observation laboratory (RU-COOL) advanced modeling system developed to cost-effectively support offshore wind energy development and operational applications. MTS/IEEE Oceans 2012, 4 pp.
- [2] Haller, George. "Lagrangian coherent structures." Annual Review of Fluid Mechanics 47 (2015): 137-162.